Ion polished Cr/Sc attosecond multilayer mirrors for high water window reflectivity

Alexander Guggenmos,[1,2,*] Stefan Radünz,[1,2] Roman Rauhut,[1,2] Michael Hofstetter,[1,2] Sriram Venkatesan,[3,4] Angela Wochnik,[3] Eric M. Gullikson,[5] Stefan Fischer,[1,6] Bert Nickel,[1,6] Christina Scheu,[3,4] and Ulf Kleineberg[1,2]

[1]*Ludwig-Maximilians-Universität München, Fakultät für Physik, Am Coulombwall 1, D-85748 Garching, Germany*
[2]*Max-Planck-Institut für Quantenoptik, Hans-Kopfermann-Straße 1, D-85748 Garching, Germany*
[3]*Ludwig-Maximilians-Universität München, Department Chemie, Butenandstraße 5-13, D-81377 München, Germany*
[4]*Current Address: Max-Planck-Institut für Eisenforschung GmbH, Max-Planck-Str. 1, D-40237 Düsseldorf, Germany*
[5]*Center for X-Ray Optics, Lawrence Berkeley National Lab 2-400, 1 Cyclotron Road, Berkeley, CA 94720, USA*
[6]*Center for NanoScience, Ludwig-Maximilians-Universität München, Schellingstraße 4, D-80799 München, Germany*
[*]*alexander.guggenmos@physik.uni-muenchen.de*

Abstract: Recent advances in the development of attosecond soft X-ray sources ranging into the water window spectral range, between the 1s states of carbon and oxygen (284 eV–543 eV), are also driving the development of suited broadband multilayer optics for steering and shaping attosecond pulses. The relatively low intensity of current High Harmonic Generation (HHG) soft X-ray sources calls for an efficient use of photons, thus the development of low-loss multilayer optics is of uttermost importance. Here, we report about the realization of broadband Cr/Sc attosecond multilayer mirrors with nearly atomically smooth interfaces by an optimized ion beam deposition and assisted interface polishing process. This yields to our knowledge highest multilayer mirror reflectivity at 300 eV near normal incidence. The results are verified by transmission electron microscopy (TEM) and soft/hard X-ray reflectometry.

OCIS codes: (230.4170) Multilayers; (340.7480) X-rays, soft x-rays, extreme ultraviolet (EUV); (240.5770) Roughness; (230.4040) Mirrors; (310.1860) Deposition and fabrication; (320.0320) Ultrafast optics.

References and links

1. Ch. Spielmann, N. H. Burnett, S. Sartania, R. Koppitsch, M. Schnürer, C. Kan, M. Lenzner, P. Wobrauschek, and F. Krausz, "Generation of coherent X-rays in the water window using 5-femtosecond laser pulses," Science **278**(5338), 661–664 (1997).
2. F. Eriksson, G. A. Johansson, H. M. Hertz, E. M. Gullikson, U. Kreissig, and J. Birch, "14.5% near-normal incidence reflectance of Cr/Sc x-ray multilayer mirrors for the water window," Opt. Lett. **28**(24), 2494–2496 (2003).
3. T. Kuhlmann, S. Yulin, T. Feigl, N. Kaiser, T. Gorelik, U. Kaiser, and W. Richter, "Chromium-scandium multilayer mirrors for the nitrogen K_α line in the water window region," Appl. Opt. **41**(10), 2048–2052 (2002).
4. F. Eriksson, N. Ghafoor, L. Hultman, and J. Birch, "Reflectivity and structural evolution of Cr/Sc and nitrogen containing Cr/Sc multilayers during thermal annealing," J. Appl. Phys. **104**(6), 063516 (2008).
5. A. I. Fedorenko, V. V. Kondratenko, Yu. P. Pershin, O. V. Poltseva, E. N. Zubarev, L. L. Balakireva, V. V. Didyk, and V. V. Burtsev, "Structure and optical properties of multilayer X-ray mirrors for long wave part (3.1-4.4 nm) of "water window"," Cryst. Res. Technol. **29**(8), 1139–1147 (1994).
6. T. Gorniak, R. Heine, A. P. Mancuso, F. Staier, C. Christophis, M. E. Pettitt, A. Sakdinawat, R. Treusch, N. Guerassimova, J. Feldhaus, C. Gutt, G. Grübel, S. Eisebitt, A. Beyer, A. Gölzhäuser, E. Weckert, M. Grunze, I. A. Vartanyants, and A. Rosenhahn, "X-ray holographic microscopy with zone plates applied to biological samples in the water window using 3rd harmonic radiation from the free-electron laser FLASH," Opt. Express **19**(12), 11059–11070 (2011).
7. W. Chao, J. Kim, S. Rekawa, P. Fischer, and E. H. Anderson, "Demonstration of 12 nm resolution Fresnel zone plate lens based soft X-ray microscopy," Opt. Express **17**(20), 17669–17677 (2009).
8. T. Salditt and T. Ducic, "X-ray microscopy for neuroscience: novel opportunities by coherent optics," in *Super-Resolution Microscopy in the Neurosciences*, E. F. Fornasiero and S. O. Rizzoli, eds. (Humana, 2014).

#220961 - $15.00 USD Received 14 Aug 2014; revised 2 Oct 2014; accepted 2 Oct 2014; published 20 Oct 2014

9. M. Schultze, M. Fiess, N. Karpowicz, J. Gagnon, M. Korbman, M. Hofstetter, S. Neppl, A. L. Cavalieri, Y. Komninos, T. Mercouris, C. A. Nicolaides, R. Pazourek, S. Nagele, J. Feist, J. Burgdörfer, A. M. Azzeer, R. Ernstorfer, R. Kienberger, U. Kleineberg, E. Goulielmakis, F. Krausz, and V. S. Yakovlev, "Delay in photoemission," Science **328**(5986), 1658–1662 (2010).
10. A. J. Verhoef, A. V. Mitrofanov, X. T. Nguyen, M. Krikunova, S. Fritzsche, N. M. Kabachnik, M. Drescher, and A. Baltuška, "Time-and-energy-resolved measurement of Auger cascades following Kr 3d excitation by attosecond pulses," New J. Phys. **13**(11), 113003 (2011).
11. M. Santos-Lleo, N. Schartel, H. Tananbaum, W. Tucker, and M. C. Weisskopf, "The first decade of science with Chandra and XMM-Newton," Nature **462**(7276), 997–1004 (2009).
12. D. Martínez-Galarce, R. Soufli, D. L. Windt, M. Bruner, E. Gullikson, S. Khatri, E. Spiller, J. C. Robinson, S. Baker, and E. Prast, "Multisegmented, multilayer-coated mirrors for the Solar Ultraviolet imager," Opt. Eng. **52**(9), 095102 (2013).
13. M. Hofstetter, A. Aquila, M. Schultze, A. Guggenmos, S. Yang, E. Gullikson, M. Huth, B. Nickel, J. Gagnon, V. S. Yakovlev, E. Goulielmakis, F. Krausz, and U. Kleineberg, "Lanthanum-molybdenum multilayer mirrors for attosecond pulses between 80 and 130 eV," New J. Phys. **13**(6), 063038 (2011).
14. M. Suman, G. Monaco, M.-G. Pelizzo, D. L. Windt, and P. Nicolosi, "Realization and characterization of an XUV multilayer coating for attosecond pulses," Opt. Express **17**(10), 7922–7932 (2009).
15. C. Liu, Z. Zeng, R. Li, Z. Xu, and M. Nisoli, "Attosecond photoionization for reconstruction of bound-electron wave packets," Phys. Rev. A **90**(1), 013403 (2014).
16. G. Sansone, F. Kelkensberg, J. F. Pérez-Torres, F. Morales, M. F. Kling, W. Siu, O. Ghafur, P. Johnsson, M. Swoboda, E. Benedetti, F. Ferrari, F. Lépine, J. L. Sanz-Vicario, S. Zherebtsov, I. Znakovskaya, A. L'Huillier, M. Yu. Ivanov, M. Nisoli, F. Martín, and M. J. J. Vrakking, "Electron localization following attosecond molecular photoionization," Nature **465**(7299), 763–766 (2010).
17. L. Belshaw, F. Calegari, M. J. Duffy, A. Trabattoni, L. Poletto, M. Nisoli, and J. B. Greenwood, "Ultrafast electron dynamics in an amino acid measured by attosecond pulses," in *The European Conference on Lasers and Electro-Optics* (Optical Society of America, 2013), paper CFIE_1.
18. T. Popmintchev, M.-C. Chen, D. Popmintchev, P. Arpin, S. Brown, S. Ališauskas, G. Andriukaitis, T. Balciunas, O. D. Mücke, A. Pugzlys, A. Baltuška, B. Shim, S. E. Schrauth, A. Gaeta, C. Hernández-García, L. Plaja, A. Becker, A. Jaron-Becker, M. M. Murnane, and H. C. Kapteyn, "Bright coherent ultrahigh harmonics in the keV X-ray regime from mid-infrared femtosecond lasers," Science **336**(6086), 1287–1291 (2012).
19. M. Schultze, A. Wirth, I. Grguras, M. Uiberacker, T. Uphues, A. J. Verhoef, J. Gagnon, M. Hofstetter, U. Kleineberg, E. Goulielmakis, and F. Krausz, "State-of-the-art attosecond metrology," J. Electron Spectrosc. Relat. Phenom. **184**(3), 68–77 (2011).
20. K. Varjú, P. Johnsson, R. López-Martens, T. Remetter, E. Gustafsson, J. Mauritsson, M. B. Gaarde, K. J. Schafer, Ch. Erny, I. Sola, A. Zaïr, E. Constant, E. Cormier, E. Mével, and A. L'Huillier, "Experimental studies of attosecond pulse trains," Laser Phys. **15**(6), 888–898 (2005).
21. F. Schäfers, H.-C. Mertins, F. Schmolla, I. Packe, N. N. Salashchenko, and E. A. Shamov, "Cr /Sc multilayers for the soft-x-ray range," Appl. Opt. **37**(4), 719–728 (1998).
22. C. T. Horovitz, *Scandium Its Occurrence, Chemistry Physics, Metallurgy, Biology and Technology* (Academic, 1975).
23. L. Névot and P. Croce, "Caractérisation des surfaces par réflexion rasante de rayons X. Application à l'étude du polissage de quelques verres silicates," Rev. Phys. Appl. (Paris) **15**(3), 761–779 (1980).
24. E. M. Gullikson, F. Salmassi, A. L. Aquila, and F. Dollar, "Progress in short period multilayer coatings for water window applications," http://www.osti.gov/bridge/servlets/purl/932470-IG3P4J/932470.pdf.
25. M. Prasciolu, A. F. G. Leontowich, K. R. Beyerlein, and S. Bajt, "Thermal stability studies of short period Sc/Cr and Sc/B4C/Cr multilayers," Appl. Opt. **53**(10), 2126–2135 (2014).
26. E. Ziegler, L. Peverini, N. Vaxelaire, A. Cordon-Rodriguez, A. Rommeveaux, I. V. Kozhevnikov, and J. Susini, "Evolution of surface roughness in silicon X-ray mirrors exposed to a low-energy ion beam," Nucl. Instrum. Methods Phys. Res. Sect. A **616**(2), 188–192 (2010).
27. A. Guggenmos, R. Rauhut, M. Hofstetter, S. Hertrich, B. Nickel, J. Schmidt, E. M. Gullikson, M. Seibald, W. Schnick, and U. Kleineberg, "Aperiodic CrSc multilayer mirrors for attosecond water window pulses," Opt. Express **21**(19), 21728–21740 (2013).
28. M. Hofstetter, M. Schultze, M. Fiess, B. Dennhardt, A. Guggenmos, J. Gagnon, V. S. Yakovlev, E. Goulielmakis, R. Kienberger, E. M. Gullikson, F. Krausz, and U. Kleineberg, "Attosecond dispersion control by extreme ultraviolet multilayer mirrors," Opt. Express **19**(3), 1767–1776 (2011).
29. C. Bourassin-Bouchet, M. Stephens, S. de Rossi, F. Delmotte, and P. Chavel, "Duration of ultrashort pulses in the presence of spatio-temporal coupling," Opt. Express **19**(18), 17357–17371 (2011).
30. C. Bourassin-Bouchet, S. de Rossi, J. Wang, E. Meltchakov, A. Giglia, N. Mahne, S. Nannarone, and F. Delmotte, "Shaping of single-cycle sub-50-attosecond pulses with multilayer mirrors," New J. Phys. **14**(2), 023040 (2012).
31. J. F. Ziegler, M. D. Ziegler, and J. P. Biersack, "SRIM – the stopping and range of ions in matter (2010)," Nucl. Instrum. Methods Phys. Res. Sect. B **268**(11), 1818–1823 (2010).
32. G. K. Hubler and J. A. Sprague, "Energetic particles in PVD technology: particle-surface interaction processes and energy-particle relationships in thin film deposition," Surf. Coat. Tech. **81**(1), 29–35 (1996).
33. C. M. Gilmore and J. A. Sprague, "Interface mixing of energetic metals deposited onto metals," Surf. Coat. Tech. **83**(1), 146–150 (1996).
34. B. L. Henke, E. M. Gullikson, and J. C. Davis, "X-ray interactions: photoabsorption, scattering, transmission, and reflection at E=50-30000 eV, Z=1-92," At. Data Nucl. Data Tables **54**(2), 181–342 (1993).

#220961 - $15.00 USD Received 14 Aug 2014; revised 2 Oct 2014; accepted 2 Oct 2014; published 20 Oct 2014

35. S. A. Yulin, T. Kuhlmann, T. Feigl, and N. Kaiser, "Reflectivity and stability of Cr/Sc multilayers for the soft x-ray range," Proc. SPIE **4782**, 285–291 (2002).
36. R. Gavrila, A. Dinescu, and D. Mardare, "A power spectral density study of thin films morphology based on AFM profiling," Rom. J. Inf. Sci. Tech. **10**(3), 291–300 (2007).
37. E. I. Gladyshevskii and E. I. Émes-Misenko, "Crystal structures of silicon-rich scandium and yttrium silicides," Zh. Strukt. Khim. **4**(6), 861–864 (1963).
38. A. B. Gokhale and G. J. Abbaschian, "The Sc-Si (scandium-silicon) system," Bull. Alloy Phase Diagrams **7**(4), 333–336 (1986).
39. PXRMS Multilayer Survey, http://henke.lbl.gov/multilayer/survey.html
40. E. Spiller, *Soft X-ray optics* (SPIE Optical Engineering Press, 1994).
41. U. Kleineberg, "New routes towards even shorter attosecond soft X-ray pulses," Ann. Phys. **525**(12), A188–A190 (2013).
42. K. Zhao, Q. Zhang, M. Chini, Y. Wu, X. Wang, and Z. Chang, "Tailoring a 67 attosecond pulse through advantageous phase-mismatch," Opt. Lett. **37**(18), 3891–3893 (2012).
43. E. Goulielmakis, M. Schultze, M. Hofstetter, V. S. Yakovlev, J. Gagnon, M. Uiberacker, A. L. Aquila, E. M. Gullikson, D. T. Attwood, R. Kienberger, F. Krausz, and U. Kleineberg, "Single-cycle nonlinear optics," Science **320**(5883), 1614–1617 (2008).

1. Introduction

Highly reflective multilayer mirrors for the water window spectral range, the spectral range defined by the K-edges of carbon and oxygen (284 eV and 543 eV, respectively) [1], have become of great interest over the last decades [2–5]. The water window serves as almost perfect spectral range for the investigation of biological processes as the carbon atoms of tissue are highly absorbing, while their natural aqueous environment is transparent in comparison. Various applications are aiming for physical access to biologically relevant processes, like high-resolution microscopy [6–8], time-resolved attosecond (soft) X-ray spectroscopy [9,10] or (X-ray) astronomy [11,12]. These applications demand multilayer mirrors for beam steering, spectral shaping or as focusing elements. Low photon loss can be accomplished by accurate deposition processes and lowest interface imperfections of such mirrors. Here we focus on the extension of mirror technology for attosecond (1 as = 10^{-18} s) pulses from currently sub-200 eV [13,14] to the water window spectral range. This will provide not only new insight into the dynamics of ultrafast core-shell electron wave packets [15], measured by time-resolved spectroscopy, but will also push forward the investigation of biomolecules and cells in attosecond time-resolved soft X-ray microscopy experiments [16,17]. The dominating generation process for attosecond pulses is High Harmonic Generation (HHG) in gases, ranging to the keV region [18]. However, the available photon numbers are, especially for low cross section experiments [19,20], not sufficiently high and thus demand high reflectivity optics. The most appropriate multilayer material combination in the lower spectral half of the water window up to about 400 eV, is chromium (Cr) and scandium (Sc) [21]. The highest reflectivity can be achieved in the vicinity of the Sc L_3-absorption edge (≈398 eV). This material combination has no overlap in the phase diagram, thus no alloys are formed [22] which theoretically facilitates an almost perfectly abrupt interface. Periodic multilayers in the water window have layer thicknesses of only 1–2 nm and the reflectivity is strongly influenced by the interface roughness σ. Throughout this manuscript the most common model for the interface roughness is being used: The *Nevot-Croce* factor takes into account the respective index of refraction *n* and the respective propagation grazing angle θ of radiation of wavelength λ from material 1 to material 2 [23]:

$$R = R_0 \exp\left[-n_1 n_2 \sin\theta_1 \sin\theta_2 \left(\frac{4\pi\sigma}{\lambda}\right)^2\right]. \quad (1)$$

Here R_0 is the reflectance of an ideal structure with interface roughness σ = 0 nm. According to Eq. (1) interface imperfections have a great influence on the reflectivity. Besides the possibility of using barrier layers like boron carbide (B_4C) [24,25], one can minimize the interface roughness by manipulation of the interface roughness evolution [26] during the layer-by-layer growth by optimization of the deposition process as being proven within this manuscript.

#220961 - $15.00 USD Received 14 Aug 2014; revised 2 Oct 2014; accepted 2 Oct 2014; published 20 Oct 2014

Here, we report about our achievements in minimizing the interface roughness of ion beam deposited Cr/Sc multilayer mirrors by optimizing the kinetic energy of sputtering krypton (Kr) ions but also by the assisted ion beam interface polishing process.

2. Methodology and mirror parameters

2.1 Dual ion beam deposition system

All mirrors were produced using a dual ion beam load-locked deposition machine at a constant background pressure of 10^{-9} mbar. A detailed explanation of the setup can be found in Guggenmos et al. [27]. Inside the two radio frequency inductively-coupled ion beam sources, ultrahigh purity krypton (99.999%) gas is ionized and the ions are accelerated by means of the applied sputtering grid voltage, either towards the selected target material (deposition plasma source) or directly towards the substrate (assist plasma source). Using krypton as process gas instead of argon (Ar), offers a lower sputter yield and a lower kinetic energy for chromium and scandium, thus enables a better control over the deposition process. The krypton ions are neutralized directly after leaving the sources by an extra electron source to prevent the targets and substrates from charging effects, which might result in fluctuating deposition rates. Layer thicknesses are controlled over sputter times. These times are being calculated from material-dependent bulk sputtering rates. The model takes into account diffusion, height factors and additional process parameters, such as shutter response time. Typical deposition rates for chromium and scandium are in the range of 0.035–0.05 nm/s, dependent on the material and the applied sputter voltage. For the purpose of the carried out examinations, the multilayer stacks were deposited on crystalline Si (100) wafers with a native SiO_2 layer of approximately two nanometers, as previous ellipsometry measurements revealed [27].

2.2 Defining optimized deposition parameters

We have composed three different sets of deposition parameters, referred to as *default*, *optimized* and *optimized + assist*. Please note that due to the stability of the ion sources and thus the deposition process, one prefers to work with the same deposition parameters throughout the complete fabrication process of one mirror. The *default* parameter set includes deposition parameters which have been previously optimized for material systems suitable for attosecond multilayer mirrors beyond 200 eV, like silicon (Si), molybdenum (Mo), lanthanum (La) or boron carbide (B_4C) [13,28–30]. For the *optimized* sets we refined the deposition of chromium and scandium in terms of kinetic energy. Refinement of deposition parameters has been based on Monte-Carlo simulations using the software SRIM [31]. Thereby the best trade-off between the optimum kinetic energy of the sputtered atoms for an optimized layer growth of defect-free, dense, smooth layers [32] and a low penetration depth into the subjacent layer to prevent layer intermixing [33] was identified. We have simulated the kinetic energy of the target atoms (Cr and Sc) in dependence on the kinetic energy of the krypton ions. From those results the penetration depth at the interface was deduced. Both results are depicted in Fig. 1. We have set a value of 10 eV as optimal kinetic energy to ensure an optimized layer growth. Our *default* process parameter set uses 600 eV krypton ions, which results in kinetic energies of the sputtered chromium atoms slightly below 10 eV, but with a rather large penetration depth into the underlying scandium layer of ~0.55 nm. The kinetic energy for krypton in the *optimized* parameter set was determined to be 400 eV to ensure a kinetic energy slightly below 10 eV for scandium as well and to reduce additionally for both materials the penetration depth in each other at the interfaces.

#220961 - $15.00 USD Received 14 Aug 2014; revised 2 Oct 2014; accepted 2 Oct 2014; published 20 Oct 2014

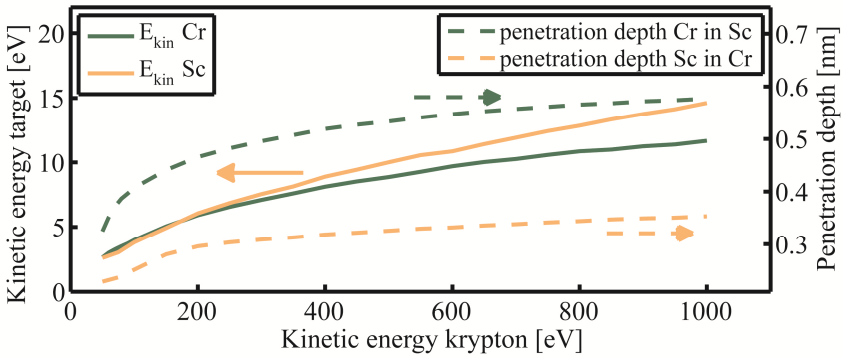

Fig. 1. Monte-Carlo simulated kinetic energy (solid lines) and penetration depth (dashed lines) at the interface for chromium (green) and scandium (orange) atoms dependent on the kinetic energy of the krypton ions.

The last parameter set, *optimized + assist*, is identical to the parameter set *optimized*, with one important difference: the assist plasma source was used for ion polishing on every 10th Cr layer, thus after every 10th period. Previous profilometry measurements showed that no loss in height is caused by the polishing process with the chosen parameters and only surface smoothing occurs. The polishing step was realized with krypton ions accelerated towards the substrate under 31 degree normal incidence with a kinetic energy of 50 eV for 60 seconds. This kinetic energy ensures an almost vanishing sputter yield (≈0.01 atoms/ion) and a low penetration depth of approximately 0.5 nm compared to a typical layer thickness of more than 1 nm. Please note that although scandium shows an even smaller sputter yield (≈0.003 atoms/ion), the larger penetration depth (≈0.95 nm) of 50 eV krypton ions leads to more krypton implantation. Therefore, we have considered chromium as the suitable polishing layer. Both the repetition (every 10th period) and the duration (for 60 seconds) of the polishing step, have been chosen as a trade-off between the overall deposition time and the smoothing effect since working with two plasma sources introduces additional ramping and parameter stabilization steps and we did not expect a high degree of interface roughness accumulation during a 10 period growth in contrast to an 80 period growth, which is confirmed in the results section.

2.3 Multilayer mirror design

Please note that throughout this manuscript, reflectivity simulations and reflectivity fits have been performed using a self-written multilayer Fresnel code. Tabulated values of the atomic scattering factors from Henke and Gullikson [34] for Cr and Sc have been used and bulk layer densities have been assumed.

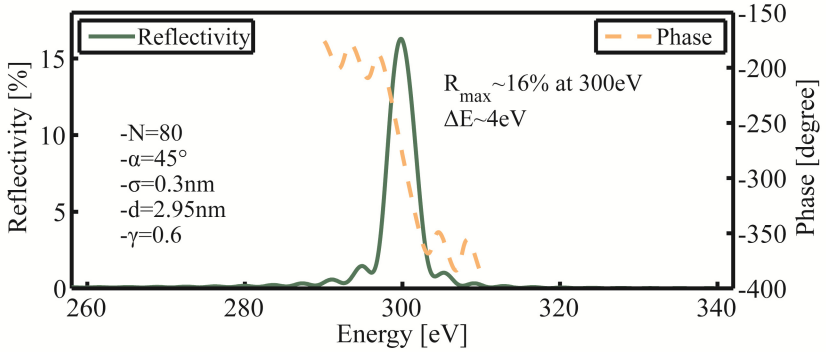

Fig. 2. Soft X-ray simulation of the reflectivity (green solid) and phase (orange dashed) with the selected mirror parameters indicated at the left.

#220961 - $15.00 USD Received 14 Aug 2014; revised 2 Oct 2014; accepted 2 Oct 2014; published 20 Oct 2014

As future attosecond sources are likely to generate a usable number of photons first of all in the lower energy range of the water window, periodic mirrors were designed for a central energy of 300 eV and a FWHM bandwidth of 4 eV at an angle of incidence of 45 degree (Fig. 2). The mirror parameters were chosen as a trade-off between a high number of interfaces, thus a high degree of analyzable roughness evolution and a high peak reflectivity, but also supporting the broadband reflection of sub-500 attosecond pulses. We utilized the three sets of deposition parameters for the fabrication of periodic Cr/Sc multilayer mirrors with a period number of N = 80, a period thickness of d = 2.95 nm and a gamma factor of $\gamma = 0.6$ ($d_{Sc}/(d_{Sc} + d_{Cr})$), resulting in individual layer thicknesses for chromium and scandium of 1.18 nm and 1.77 nm, respectively. Simulations reveal a peak reflectivity of ~16% when an interface roughness of $\sigma = 0.3$ nm is assumed. Current state of the art Cr/Sc multilayer mirrors with interface roughness values of $\sigma = 0.31–0.35$ nm have been achieved by magnetron sputtering deposition [35] with quasi single-atomic barrier layers [24,25] to prevent interdiffusion. Our goal is to decrease the interface roughness without barrier layers from $\sigma \approx 0.5$ nm [27] and achieve comparable or better interface quality than current state of the art values. This should be realized by ion beam deposition plus recurring ion polishing, because the ion polishing process can be better controlled than the barrier layer deposition, thus resulting in a better multilayer structure accuracy.

3. Analysis methods and results

3.1 Stability of the deposition process by profilometry

To prove the accuracy and the stability of the deposition process, we have measured the total stack height after the deposition by surface profilometry and compared it to the theoretical value. Simulations revealed a theoretical total stack height of 237.1 nm (including the top chromium oxide layer). We could experimentally confirm this by surface profilometry with a measured total stack thickness of (237.4 ± 0.9) nm for all three samples.

3.2 Characterization by hard X-ray reflectometry

Hard X-ray reflectometry (XRR), using a molybdenum K_α source with a wavelength of $\lambda \approx 0.071$ nm, was performed. A comparison of the measured XRR data of the three mirrors is shown in Fig. 3.

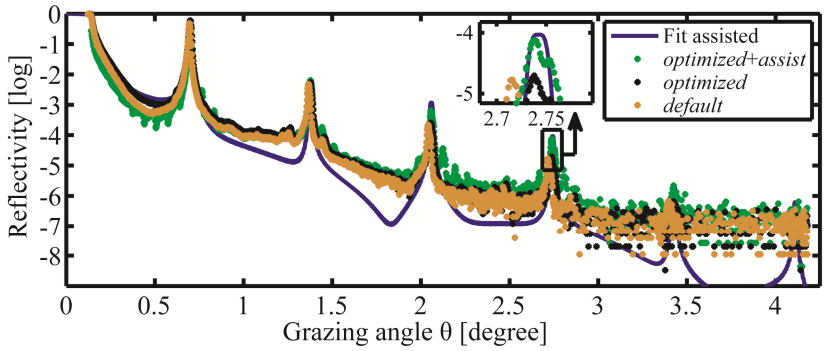

Fig. 3. Hard X-ray reflectometry data for the three different mirrors. The lowest interface roughness, thus the highest peak intensities, shows the *optimized + assist* mirror. Only the fit of the interface polished mirror is shown.

When comparing the intensities of the higher order Bragg peaks, where the impact of interface roughness is high, one can clearly see the improvement caused by the tailoring of the deposition parameters. While the *default* and the *optimized* stack reveal similar reflectivity e.g. in the 4th order Bragg peak (inset in Fig. 3) a more than 5 times higher reflectivity could be revealed in the *optimized + assist* stack. Out of the fitting procedure for each measurement, we obtained a mean interface roughness value of $\sigma = 0.26$ nm for the *default*, $\sigma = 0.24$ nm for

#220961 - $15.00 USD Received 14 Aug 2014; revised 2 Oct 2014; accepted 2 Oct 2014; published 20 Oct 2014

the *optimized* and σ = 0.21 nm for the *optimized* + *assist* parameter set with a 0.01 nm error range.

3.3 Characterization by transmission electron microscopy

TEM investigations were carried out using a FEI Titan 80-300 TEM/STEM field emission TEM operated at 300 kV, equipped with an EDAX detector for energy dispersive X-ray spectroscopy and a Gatan Tridiem image filter for electron energy loss spectroscopy measurements. For high angle annular dark field (HAADF) imaging in scanning TEM (STEM) mode a detector from Fischione Instruments (Model 3000) is attached. Conventional TEM cross section specimens were prepared by cutting, gluing into a brass holder, slicing, grinding, dimpling and double-sided Ar ion beam milling at 5 degree and 4 keV. The latter was performed until a physical hole was achieved using a liquid nitrogen cooled, precision ion polishing system (Gatan Model 491).

TEM cross section measurements were carried out on witness samples grown on Si (100). Their period number of N = 80 and their small period thickness of d = 2.95 nm made these coatings perfectly suited for TEM analysis. TEM images of the coatings are shown in Fig. 4.

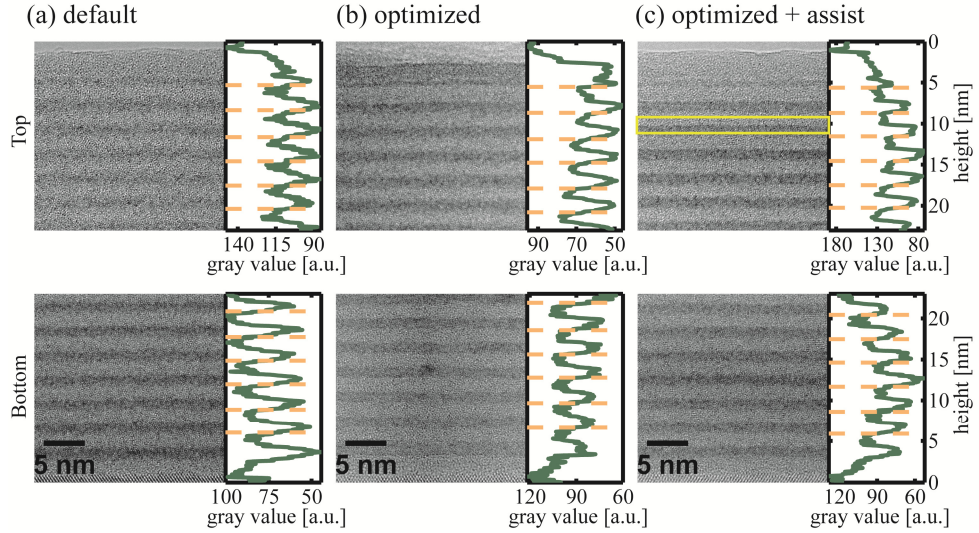

Fig. 4. TEM cross section images of the multilayer evolution from bottom (lower panel) to top (upper panel) with the *default* (left column), *optimized* (center column) and *optimized* + *assist* parameters including the assisted interface polishing (right column). The images show a multilayer detail of 23 nm x 23 nm with a 5 nm scale bar in the bottom images. Next to each image the lineouts of the gray value analysis is shown. More information can be found in the text.

The upper row displays the top six periods of each coating (topmost layer is assumed to be Cr_2O_3 [27]) and the lower row shows the seven bottom periods of each stack close to the substrate interface beginning with the Sc layer. The top and bottom layers were chosen for investigation because if changes occur they will be more pronounced at these regions. Alternating bright and dark layers, observed in the TEM images, corresponds to scandium and chromium respectively which has also been verified using HAADF imaging in scanning TEM mode. Necessary care has been taken during TEM specimen preparation and image acquisition that change in thickness or focus is not responsible for the observed effects. Please note that the images of Fig. 4 show TEM raw data, thus unprocessed contrast data. From TEM data we observed films that are almost complete amorphous nanolayers with an occasional nanocrystalline phase. Therefore we do not observe electron diffraction on polycrystalline layers, but measure charge density dependent data instead.

#220961 - $15.00 USD Received 14 Aug 2014; revised 2 Oct 2014; accepted 2 Oct 2014; published 20 Oct 2014

For the *default* parameter set (Fig. 4, left column), layers are clearly distinguishable at the bottom of the stack (Fig. 4(d)) whereas they show a significant degree of intermixing at the top (Fig. 4(a)) which is determined on basis of the diminishing layer contrast. With the *optimized* parameter set the layers at the bottom and the top (Fig. 4, center column) are comparable with regard to image contrast, while for the additionally polished multilayer the layers at the top (Fig. 4(c)) seem to show even a decreased intermixing and increased layer-to-layer interface abruptness. We have additionally evaluated the averaged gray values (parallel to the interface) along the 23 nm x 23 nm unprocessed TEM images to visualize the interface between the layers. The corresponding lineouts are depicted next to each image. The bottom periods are almost comparable since a high difference in roughness evolution is not expected for the first starting periods. This is different at the top periods. For the *default* parameter set a strong zig-zag pattern occurs, indicating a worsened interface roughness whereas for the *optimized* set a transition to a more sinusoidal lineout occurs. In case of the polished mirror we even observe an almost rectangular profile with flat plateaus at the bottom and the top, indicating very well separated layers with lowest interface roughness. In summary, the best layer characteristics and stack evolution has been achieved by optimized kinetic deposition energy and chromium layer ion polishing of every tenth period, resulting in clearly distinguishable layers, both at the bottom and at the top of the stack, and significantly improved layer-to-layer interfaces without roughness accumulation over an eighty period stack.

For a more quantitative insight into the stack evolution, we have determined the Power Spectral Density (PSD) [36] and calculated the resultant interface roughness σ:

$$\sigma = \left(\int_{f_{min}}^{f_{max}} \mathrm{PSD}(f_x) \mathrm{d}f_x \right)^{1/2}. \qquad (2)$$

The small yellow rectangle of Fig. 4(c) is shown enlarged in Fig. 5(a).

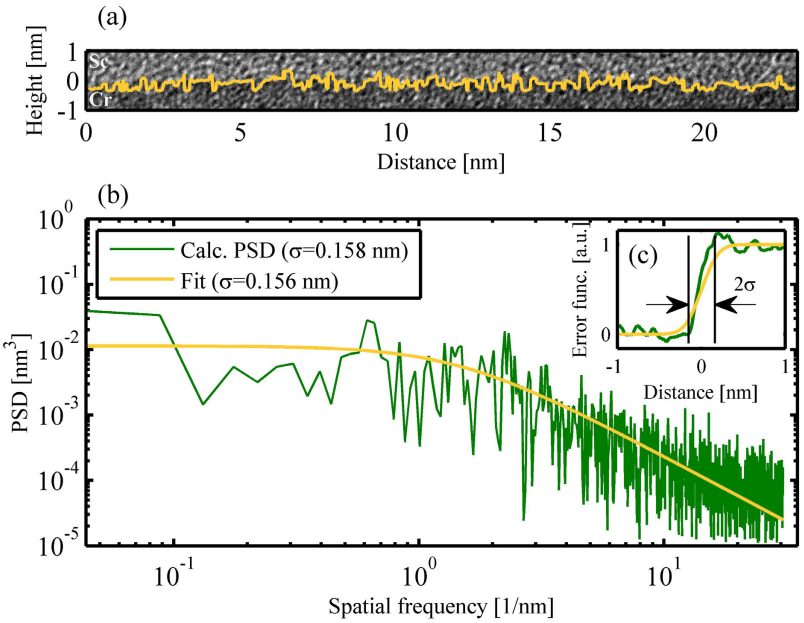

Fig. 5. (a) Enlarged interface of scandium on top of chromium together with the interface transition (orange), which was determined by a self-written contrast analyzer code. (b) Corresponding calculated PSD (green) together with the fit and the obtained interface roughness values. These results correspond to the selected interface of the *optimized* + *assist* multilayer mirror, which is depicted as yellow rectangle in Fig. 4(c). (c) Shows the averaged height profile along the 23 nm length (green) together with an error function defined by the PSD fitted roughness value (orange).

#220961 - $15.00 USD Received 14 Aug 2014; revised 2 Oct 2014; accepted 2 Oct 2014; published 20 Oct 2014

Using a self-written contrast analyzer code, we have determined the pixel position where the transition from one material to the other occurs. We have averaged 0.2 nm (13 pixel as a trade-off between resolving the PSD and not addressing too high frequency components) neighbor pixels along the 23 nm (1410 pixel) distance (parallel to the interface) as well as 0.65 nm (40 pixel) in the scandium and chromium regime (along the layer growth) to determine the mean plateau value in the central layer region, to prevent a wrong data analysis due to intensity fluctuations which occur in TEM measurements. This simplified approach leads to the yellow height profile in Fig. 5(a), which describes the interface. For the one dimensional case, where the topography of a profile describes its height z(x), the PSD is defined by:

$$\mathrm{PSD}(f_x) \approx L\left[\frac{1}{N}\sum_{k=1}^{N} z_k \cdot \exp\left(2\pi i \cdot x_k \cdot f_x\right)\right]^2, \qquad (3)$$

with the length position $x_k = k \bullet L/N$ and the spatial frequencies $f_x = j/L$, $j = 1,2,\ldots,N/2$. The calculated and fitted PSD according to Eq. (3) is shown in Fig. 5(b) for the interface section in Fig. 5(a). For the interface of scandium on top of chromium we calculate from Eq. (2) an interface roughness of $\sigma = 0.158 \pm 0.005$ nm and get a fitted value of $\sigma = 0.156 \pm 0.005$ nm. Finally, we compare our PSD results, where each pixel contributes to the roughness value, against the averaged height profile of the lineout in Fig. 4. The comparison of the averaged height profile with the error function being defined by the fitted PSD roughness value is depicted in 5(c). We find a good agreement. This result proves the robustness of our analysis methods.

To get a quantitative insight on the roughness evolution in the stacks with better statistics, dependent on the deposition parameters and on the order of the interfaces (i.e. from chromium to scandium and vice versa), we have determined the interface roughness value for each interface for the six TEM cross sections shown in Fig. 4. The results are shown in Table 1. We distinguish between the bottom and the top periods, the order of the interface as well as the used deposition parameter set. Please note that due to the diminishing layer contrast, the extraction of roughness values for the top interfaces of the TEM cross section in the *default* case (Fig. 4(a)) was impossible.

Table 1. Comparison of the evaluated interface roughness values σ [nm], dependent on the interface direction and the used deposition parameter set. The displayed roughness values are averaged over seven periods at the bottom and six periods at the top and take into account the error. *Default* top [] could not be evaluated.

Location	interface	*default*	*optimized*	*optimized + assist*
TOP	Cr on Sc	[]	0.33 ± 0.06	0.31 ± 0.06
	Sc on Cr	[]	0.26 ± 0.06	0.17 ± 0.04
BOTTOM	Cr on Sc	0.30 ± 0.05	0.19 ± 0.03	0.22 ± 0.06
	Sc on Cr	0.20 ± 0.06	0.16 ± 0.05	0.17 ± 0.05

The evaluated interface roughness values agree with the Monte-Carlo simulations in section 2.2. The roughness of chromium on top of scandium is higher than vice versa. This can be attributed to the higher penetration depth. A further step of improvement may be to decrease the kinetic energy of chromium to even lower values since the penetration depth of chromium in scandium seems to be the crucial parameter for the interface roughness. Finally, Fig. 6 shows a complete TEM image of the polished multilayer stack *optimized + assist* and confirms the homogeneity of the multilayer stack.

#220961 - $15.00 USD Received 14 Aug 2014; revised 2 Oct 2014; accepted 2 Oct 2014; published 20 Oct 2014

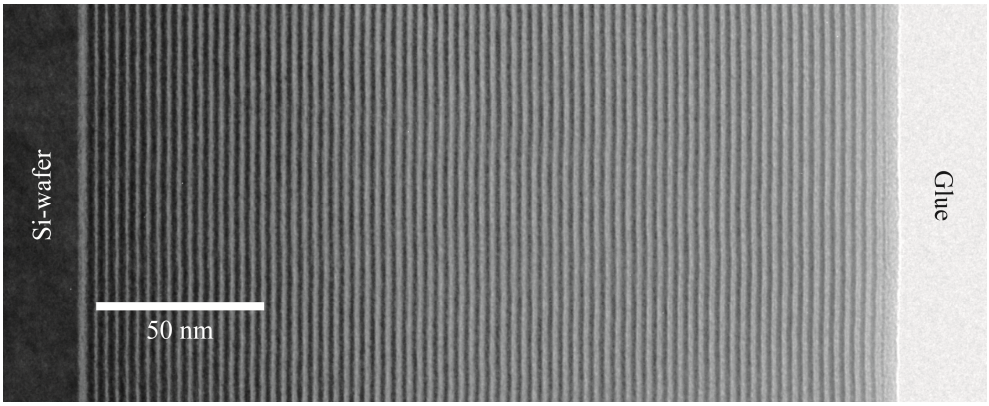

Fig. 6. TEM cross section image of the whole multilayer stack for the additional polished multilayer. Please note that the first bright layer after the Si wafer is accidentally formed by scandium silicide.

In addition to the previously shown TEM analysis results, an easy step of improvement towards an even lower interface roughness would be to start in future Cr/Sc multilayer mirrors with Cr as first layer, since our choice with Sc forms scandium silicide [37,38] as TEM analysis have shown. Therefore the good surface roughness (<0.1 nm) either of silicon wafers or fused silica substrates is lost with the first interface.

3.4 Optimization proof on high periodic mirror soft X-ray data

To finally prove the concept of optimizing the kinetic energy and ion polishing interfaces of our chromium/scandium material system, we have used as final analyzing method soft X-ray reflectometry. Measurements were done at the reflectometry beamline 6.3.2 at the Advanced Light Source and the PTB at Bessy II. To increase the impact of possible roughness accumulation on the reflectivity (Eq. (1), we have increased the period number to N = 400 and decreased the period thickness to d = 2.084 nm, thus increased the crucial σ/d-ratio. These mirrors were designed for a central energy of 300 eV but now for normal incidence with an angle of 5 degree. The result of the soft X-ray measurement for the three different deposition parameter sets is shown in Fig. 7.

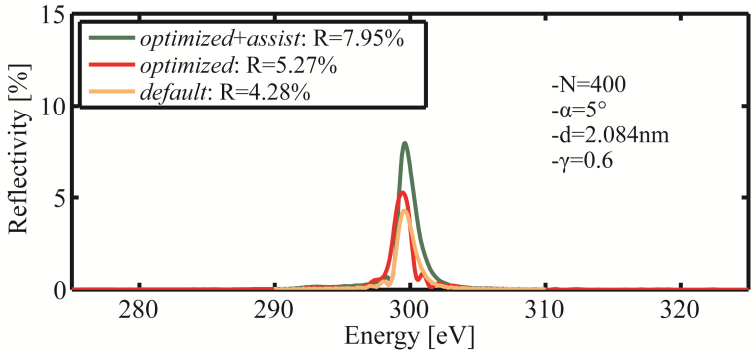

Fig. 7. Soft X-ray reflectometry measurement for the *default* (orange), *optimized* (red) and *optimized + assist* (green) set proving the right tendency of our concept. As result we achieve the highest reflectivity of ~8% in case of the additional polished multilayer mirror. The corresponding mirror parameters are depicted on the right hand side.

The soft X-ray reflectometry confirms the findings from the XRR and TEM analysis. The highest reflectivity of approximately 8% was achieved for the polished mirror. To the best of our knowledge, this is also the highest normal incidence reflectivity at a photon energy of 300 eV ever achieved [39]. The reflectivity curves have been fitted for each of the three mirrors;

#220961 - $15.00 USD Received 14 Aug 2014; revised 2 Oct 2014; accepted 2 Oct 2014; published 20 Oct 2014

the obtained roughness values are listed in Table 2. As a note to the accuracy of our fabrication process it should be mentioned that the simulated and planned center energy was 300 eV and we measured the highest reflectivity for the polished mirror at 299.6 eV, thus only with a shift of 0.13% in the center energy.

3.5 Comparison of evaluated data

The interface roughness results of the previous analysis have been summarized in Table 2.

Table 2. Comparison of the evaluated interface roughness values σ [nm], dependent on the analysis method and the used deposition parameter set. More information can be found in the text.

Method	*default*	*optimized*	*optimized + assist*
XRR	0.26	0.24	0.21
TEM	0.26	0.24	0.21
Soft X-ray	0.51	0.49	0.41

While we find identical measures from the XRR and TEM analysis, the soft X-ray values are higher. This can be partly explained by the lower penetration depth of soft X-rays in comparison to hard X-ray radiation. One finds different roughness values due to the fact that accumulated roughness as well as the interface's power spectral density [40] is weighted differently. Surface roughness for example has a minor effect on hard X-rays while it has a major impact on soft X-rays. Besides that the higher period number N as well as the lower period thickness d of the soft X-ray samples yields intrinsically higher roughness values.

4. Conclusions

We have proven the reduction of interface roughness of water window Cr/Sc multilayer mirrors by ion polishing. Broadband attosecond mirrors for the reflection of sub-500 as pulses have been fabricated. The ion beam deposited nanolayer growth was optimized by tweaking the deposition parameter of Cr/Sc multilayer mirrors, mainly by tailoring the kinetic energy of the target atoms, where the optimization was theoretically accompanied by Monte-Carlo simulations. Besides, we have realized an important step towards 'perfect' layer growth by additionally assisted ion beam interface polishing. Using a well-suited kinetic energy for the target materials (chromium and scandium) and additional interface polishing for tailored attosecond multilayer mirrors will increase the reflectivity dramatically. We have demonstrated almost atomically smooth interfaces with roughness values of $\sigma \approx 0.16$ nm. The future challenge is to realize such a value for each interface in a high-periodic normal incidence multilayer mirror and push the reflectivity to an even higher value at 300 eV for the first attosecond experiments. Such low-loss mirrors will thus enable for the first time attosecond-resolved experiments on biological samples in the water window spectral range or pave the way towards shorter pulse durations [41] than the currently achieved 67 as [42] to 80 as [43], by filtering a multi-octave cut-off spectrum from future HHG soft X-ray sources.

Acknowledgments

We thankfully acknowledge scientific support and valuable discussions by Ferenc Krausz (MPQ, LMU) and Philip Böhm (LMU) for supporting the hard X-ray measurements. This work was financially supported by the DFG via the Excellence Cluster Munich-Centre for Advanced Photonics (MAP, EXC 158).